On the Theory of a Non-Periodic Quasilattice Associated with the Icosahedral Group II*

P. Kramer
Institut für Theoretische Physik der Universität Tübingen

Z. Naturforsch. **41 a**, 897–911 (1986); received March 5, 1986

A new approach is described for a quasilattice associated with with the icosahedral group which was analyzed in Z. Naturforschung **40 a**, 775 (1985). This approach is based on dualization and intersection properties of hypercubic lattices in n dimensions. A Kepler zone is defined as a convex triacontahedron with 30 rhombus faces. The structure properties of the quasilattice are analyzed by use of this zone and by introduction of an infinite graph inside of it.

1. Introduction

The theory of non-periodic space filling developed in general in [1] was analyzed in detail in [2] for a quasilattice associated with the icosahedral group A(5). There are other quasilattices associated with the icosahedral group which are going to be studied in [3].

The present paper is a continuation of [2]. In the first part if is shown that notions of crystallography in $\mathbb{E}^n$, including p-dimensional boundaries of a cell and dualization, yield a new approach to hypercubic lattices in $\mathbb{E}^n$ projected to $\mathbb{E}^3$, and to quasilattices arising from intersections in $\mathbb{E}^n$. This analysis is presented in Sects. 2 and 3 and applied to $\mathbb{E}^6$ and projection of lattices to $\mathbb{E}^3$ in Sections 4–6.

In the second part a new analysis of the shift vector γ is developed. The results given in [2] on this vector are incomplete. The new diagnosis of the shift vector given in Sects. 7–11 employs the concept of a Kepler zone, a convex domain in $\mathbb{E}^3$ bounded by 30 rhombus faces. The analysis of the quasilattice is then presented in terms of an infinite graph K in this Kepler zone. This graph contains the full information on the quasilattice. Locally it yields the information on composite cells, on the generation of the quasilattice from a given vertex and on all matching conditions. Globally it yields the possible point symmetries and the non-periodicity and allows for the study of classification and quasiperiodic properties of the quasilattice.

---

* Work supported by Deutsche Forschungsgemeinschaft.

Reprint requests to Prof. Dr. P. Kramer, Institut für Theoretische Physik der Universität Tübingen, Auf der Morgenstelle 14, D-7400 Tübingen.

2. Hypercubic Lattices in $\mathbb{E}^n$ and Their Unit Cell

In the present section we give some general concepts for hypercubic bases and lattices in $\mathbb{E}^n$. These concepts have applications to quasilattices other than the one based on $\mathbb{E}^6$ to which we return in Sections 4–11. The discussion of these other quasilattices is implemented in [3].

As in [1], we denote by $\boldsymbol{b}_i$, $\boldsymbol{b}_j^*$, $i, j = 1, \ldots, n$ two orthogonal bases which are reciprocal to each other, that is,

$$\boldsymbol{b}_i \cdot \boldsymbol{b}_j^* = \delta_{ij}, \quad i, j = 1, \ldots, n .$$

We recall that the vectors $\boldsymbol{b}_j^*$ may be regarded as the image of the dual basis of the dual vector space V^* in V.

As in [1] we introduce a hypercubic lattice Y and a dual lattice Y^* in $\mathbb{E}^n$.

2.1. Definition: The first unit cell of the hypercubic lattice Y in $\mathbb{E}^n$ is the set of points

$$h(n; 1, \ldots, n) = \{\boldsymbol{y} \mid -\tfrac{1}{2} \leqq \boldsymbol{y} \cdot \boldsymbol{b}_i \leqq \tfrac{1}{2}, i = 1, \ldots, n\} .$$

We call a point interior to this cell if the strict inequality signs hold.

We shall study the boundaries of this cell of dimension p. The numbers k_i, $i = 1, \ldots, n$ will always take the values $k_i = \pm 1$ for this cell.

2.2. Definition: Let α: $i \to \alpha(i)$, $i = 1, \ldots, n$ denote a permutation of the numbers $1, \ldots, n$. For $j = p+1, \ldots, n$ choose $n - p$ numbers $k_{\alpha(j)} = \pm 1$. The corresponding p-boundary, $0 \leqq p \leqq n$, of the first unit cell is the set of points

$$(p; \alpha, k) = \{\boldsymbol{y} \mid -\tfrac{1}{2} \leqq \boldsymbol{y} \cdot \boldsymbol{b}_{\alpha(i)} \leqq \tfrac{1}{2}, \quad i = 1, \ldots, p; \\ \boldsymbol{y} \cdot \boldsymbol{b}_{\alpha(j)} = \tfrac{1}{2} k_{\alpha(j)}, j = p+1, \ldots, n\} .$$

0340-4811 / 86 / 0700-0897 $ 01.30/0. – Please order a reprint rather than making your own copy.

The case $p = n$ is covered by Def. 2.1. Points for which the strict inequalities hold are called interior.

2.3. Proposition: For given dimension p, the number of different p-boundaries is

$$l(p) = \binom{n}{p} 2^{n-p}.$$

The o-boundaries form the vertices of the unit cell, the 1-boundaries its edge lines, and finally the $(n-1)$-boundaries form the hyperfaces of the unit cell. The p-boundaries of the unit cell have a description in terms of the dual basis:

2.4. Proposition: Let λ_j denote real numbers with range as $-1 \leqq \lambda_j \leqq 1$, $j = 1, \ldots, n$. Then the points of the p-boundary $\hbar(p; \alpha, k)$ are given by

$$\hbar(p; \alpha, k) = \left\{ y \,\middle|\, y = \tfrac{1}{2} \sum_{i=1}^{p} \lambda_{\alpha(i)} \boldsymbol{b}^*_{\alpha(i)} + \tfrac{1}{2} \sum_{j=p+1}^{n} k_{\alpha(j)} \boldsymbol{b}^*_{\alpha(j)} \right\}.$$

For interior points the numbers λ_j are subject to the strict inequalities.

We turn now to the boundaries of a p-boundary.

2.5. Proposition: A fixed p-boundary $\hbar(p; \alpha, k)$ for $1 \leqq p \leqq n$ has $2p$ boundaries of dimension $p-1$. They are obtained by selecting an index l from $i = 1, \ldots, p$ and a number $k_{\alpha(l)} = \pm 1$ and have the points

$$y = \tfrac{1}{2} \sum_{\substack{i=1 \\ i \neq l}}^{p} \lambda_{\alpha(i)} \boldsymbol{b}^*_{\alpha(i)} + \tfrac{1}{2} k_{\alpha(l)} \boldsymbol{b}^*_{\alpha(l)} + \tfrac{1}{2} \sum_{j=p+1}^{n} k_{\alpha(j)} \boldsymbol{b}^*_{\alpha(j)}.$$

2.6. Proposition: An $(n-1)$-boundary of the first unit cell is shared with a neighbouring cell whose center is at $\boldsymbol{u} = k_{\alpha(n)} \boldsymbol{b}^*_{\alpha(n)}$.

Proof: Define the vector

$$y' = y - \boldsymbol{u}.$$

If y is a point from an $(n-1)$-boundary of the first unit cell, then

$$y' = \tfrac{1}{2} \sum_{i=1}^{n-1} \lambda_{\alpha(i)} \boldsymbol{b}^*_{\alpha(i)} - \tfrac{1}{2} k_{\alpha(n)} \boldsymbol{b}^*_{\alpha(n)}$$

is a point from some other $(n-1)$-boundary of the first unit cell, hence y is a point from an $(n-1)$-boundary of the neighbouring cell whose center is located at $\boldsymbol{u}$.

Consider now objects from the dual lattice Y^* which are dual to the boundaries of Y.

2.7. Definition: Given a p-boundary $\hbar(p; \alpha, k)$ of the unit cell of Y, associate to it the dual $(n-p)$-boundary of Y^*,

$$\hbar^*(n-p; \alpha, k) = \left\{ z \,\middle|\, z = \tfrac{1}{2} \sum_{j=p+1}^{n} \lambda_{\alpha(j)} \boldsymbol{b}_{\alpha(j)} + \tfrac{1}{2} \sum_{j=p+1}^{n} k_{\alpha(j)} \boldsymbol{b}_{\alpha(j)} \right\}.$$

In particular, the dual to the unit cell $\hbar(n; 1, \ldots, n)$ of Y is the vertex of Y^*

$$z = 0,$$

and the dual to an $(n-1)$-boundary of Y with given index $\alpha(n)$ is the line segment or edge

$$z = \tfrac{1}{2} (\lambda_{\alpha(n)} + k_{\alpha(n)}) \boldsymbol{b}_{\alpha(n)}.$$

In this dual construction, the $(p-1)$-boundaries of a p-boundary $\hbar(p; \alpha, k)$ yield

2.8. Proposition: The $2p$ duals to the $(p-1)$-boundaries of a p-boundary $\hbar(p; \alpha, k)$ have the points

$$z = \tfrac{1}{2} \lambda_{\alpha(l)} \boldsymbol{b}_{\alpha(l)} + \tfrac{1}{2} k_{\alpha(l)} \boldsymbol{b}_{\alpha(l)} + \tfrac{1}{2} \sum_{j=p+1}^{n} \lambda_{\alpha(j)} \boldsymbol{b}_{\alpha(j)} + \tfrac{1}{2} \sum_{j=p+1}^{n} k_{\alpha(j)} \boldsymbol{b}_{\alpha(j)}$$

and intersect in the $(n-p)$-boundary

$$\hbar^*(n-p; \alpha, k).$$

3. Classification of boundaries in $\mathbb{E}^n$

The full symmetry group of the hypercubic lattice Y in $\mathbb{E}^n$ is the semidirect product of the translation group T with elements $\boldsymbol{t}$ and the hyperoctahedral point group $\Omega(n)$ with elements g. We denote the elements of the space group by pairs $(\boldsymbol{t}, g)$. Now we study those subgroups of the space group which transform points from the first unit cell into points of the first unit cell. Clearly the point group $\Omega(n)$ at the origin has this property.

3.1. Proposition: The hyperoctahedral point group $\Omega(n)$ transforms the first unit cell into itself. Moreover all p-boundaries are transformed into one another under $\Omega(n)$.

Proof: The group $\Omega(n)$ contains all permutations and all reflections of the basis vectors, hence the p-boundaries form a single orbit of dimension $l(p)$.

3.2. Proposition: Define the vector

$$\boldsymbol{a} = \tfrac{1}{2} \sum_{j=p+1}^{n} k_j \boldsymbol{b}_j^*, \quad k_j = \pm 1,$$

and consider the subgroup $\Omega(p) \times \Omega(n-p)$ of $\Omega(n)$ with elements h. Here $\Omega(p)$ acts on the vectors with index $1, \ldots, p$ while $\Omega(n-p)$ acts on those with index $p+1, \ldots, n$. The elements

$$(\boldsymbol{a}, e)(0, h)(-\boldsymbol{a}, e) = (\boldsymbol{a} - h\boldsymbol{a}, h), \quad h \in \Omega(p) \times \Omega(n-p)$$

form a subgroup H of the space group.

Proof: Consider the elements of the form

$$(\boldsymbol{a}, e)(0, h)(-\boldsymbol{a}, e) = (\boldsymbol{a} - h\boldsymbol{a}, h).$$

The action of h on $\boldsymbol{a}$ is given by

$$h\boldsymbol{a} = \tfrac{1}{2} \sum_{j=p+1}^{n} k_j \varepsilon_j \boldsymbol{b}_{f(j)}^*, \quad \varepsilon_j = \pm 1$$

in the notation of [2] Section 2. Since h is an element of $\Omega(p) \times \Omega(n-p)$, we have $p+1 \leqq f(j) \leqq n$ for $p+1 \leqq j \leqq n$. Then

$$\boldsymbol{a} - h\boldsymbol{a} = \tfrac{1}{2}\left(\sum_{j=p+1}^{n} k_j \boldsymbol{b}_j^* - \sum_{j=p+1}^{n} k_j \varepsilon_j \boldsymbol{b}_{f(j)}^* \right) = \sum_{j=p+1}^{n} \tfrac{1}{2}(k_{f(j)} - k_j \varepsilon_j) \boldsymbol{b}_{f(j)}^*$$

and, since the numbers

$$k'_j = \tfrac{1}{2}(k_{f(j)} - k_j \varepsilon_j)$$

can take the values 0 or ± 1 only, $\boldsymbol{a} - h\boldsymbol{a}$ must be an element of the translation group T.

For the group just described one finds

3.3. Proposition: The group isomorphic to $\Omega(p) \times \Omega(n-p)$ described in Prop. 3.2 transforms the p-boundary $\mathscr{k}(p; e, k)$ with points

$$\boldsymbol{y} = \tfrac{1}{2} \sum_{j=p+1}^{n} k_j \boldsymbol{b}_j^* + \tfrac{1}{2} \sum_{i=1}^{p} \lambda_i \boldsymbol{b}_i^*$$

into itself.

Propositions 3.2 and 3.3 carry over to all p-boundaries. If $g \in \Omega(n)$ maps the p-boundary considered in Prop. 3.3 into a fixed p-boundary $\mathscr{k}(p; \alpha, k)$, then gHg^{-1} is a subgroup of the space group isomorphic to $\Omega(p) \times \Omega(n-p)$ and transforms $\mathscr{k}(p; \alpha, k)$ into itself. So we have

3.4. Proposition: For any p-boundary $\mathscr{k}(p; \alpha, k)$ there exists a subgroup H of the space group isomorphic to $\Omega(p) \times \Omega(n-p)$ which transforms $\mathscr{k}(p; \alpha, k)$ into itself.

4. Classification of Boundaries in $\mathbb{E}^6$ under the Icosahedral Group

The concepts of Section 2 apply in particular to the hypercubic lattice Y in $\mathbb{E}^6$. With the orthonormal basis

$$\boldsymbol{c}_i, \quad \boldsymbol{c}_i \cdot \boldsymbol{c}_j = \delta_{ij}, \quad i, j = 1, \ldots, 6$$

of [2] Section 2 we recover the same results upon putting

$$\boldsymbol{b}_i = \sqrt{2}\, \boldsymbol{c}_i, \quad \boldsymbol{b}_i^* = \sqrt{\frac{1}{2}}\, \boldsymbol{c}_i, \quad i = 1, \ldots, 6.$$

The lattice Y has the point group $\Omega(6)$, and the icosahedral group A(5) is embedded as a subgroup into $\Omega(6)$. We now restrict $\Omega(6)$ to A(5) and consider the action of A(5) on the p-boundaries of the first unit cell in $\mathbb{E}^6$. Whereas under $\Omega(6)$ all p-boundaries form a single orbit, there are several different orbits under A(5). These orbits can be listed by giving a representative and the stability group S as a subgroup of A(5). The other p-boundaries on the same orbit are then given by acting with the cosets A(5)/S on the representative. The result of this orbit analysis is given in Table 1. For given p, the center positions of the representative p-boundaries are given in terms of the numbers $k_{\alpha(j)}$ according to Def. 2.2 and Propositions 2.4.

5. Projection of the First Unit Cell to $\mathbb{E}^3$

As in [2] Sect. 2 we decompose $\mathbb{E}^6$ into the orthogonal subspaces $\mathbb{E}_1^3$ and $\mathbb{E}_2^3$ and apply this decomposition to any vector $\boldsymbol{x}$, $\boldsymbol{x} = \boldsymbol{x}_1 + \boldsymbol{x}_2$.

5.1. Definition: Let $\mathscr{k}(p; \alpha, k)$ be a p-boundary of the first unit cell in $\mathbb{E}^6$. Its projection to $\mathbb{E}_\mu^3$, $\mu = 1, 2$ is the set

$$\mathscr{k}_\mu(p; \alpha, k) = \left\{ \boldsymbol{x}_\mu \,\middle|\, \boldsymbol{x}_\mu = \tfrac{1}{2} \sum_{i=1}^{p} \lambda_{\alpha(i)} \boldsymbol{b}_{\alpha(i)\mu}^* + \tfrac{1}{2} \sum_{j=p+1}^{6} k_{\alpha(j)} \boldsymbol{b}_{\alpha(j)\mu}^* \right\}.$$

Table 1. Orbit analysis of p-boundaries for $p = 0, \ldots, 6$ under the icosahedral group A (5).

p	Orbit	Center $(k_1 k_2 k_3 k_4 k_5 k_6)$	Stability group S	$\frac{\lvert A(5) \rvert}{\lvert S \rvert}$	$l(p)$	Point group H
0	0.1	(111111)	C (5)	12		
	0.2	$(\bar{1}\bar{1}\bar{1}\bar{1}\bar{1}1)$	C (5)	12		
	0.3	$(1\bar{1}1111)$	C (3)	20		
	0.4	$(\bar{1}1\bar{1}\bar{1}\bar{1}1)$	C (3)	20	64	A (5)
1	1.1	(111110)	C (5)	12		
	1.2	$(111\bar{1}\bar{1}0)$	I	60		
	1.3	$(1\bar{1}1\bar{1}\bar{1}0)$	I	60		
	1.4	$(\bar{1}1\bar{1}\bar{1}\bar{1}0)$	I	60	192	D (5)
2	2.1	(111100)	C (2)	30		
	2.2	$(11\bar{1}\bar{1}00)$	C (2)	30		
	2.3	$(111\bar{1}00)$	I	60		
	2.4	$(1\bar{1}1100)$	I	60		
	2.5	$(1\bar{1}1\bar{1}00)$	I	60	240	D (2)
3	3.1	(000111)	C (3)	20		
	3.2	$(1\bar{1}1000)$	C (3)	20		
	3.3	$(00011\bar{1})$	I	60		
	3.4	(111000)	I	60	160	D (3)
4	4.1	(010001)	C (2)	30		
	4.2	$(01000\bar{1})$	C (2)	30	60	D (2)
5	5.1	(000001)	C (5)	12	12	D (5)
6	6.1	(000000)	A (5)	1	1	A (5)

For $p = 0, 1, 2$, this projection is a point, a line segment or a rhombus respectively. For $p \geqq 3$ one finds:

5.2. Proposition: For $p = 3, \ldots, 6$, the projection of a p-boundary is a convex polyhedron with $p(p-1)/2$ parallel pairs of rhombus faces. For two vectors $\boldsymbol{b}^*_{\alpha(r)\mu}$, $\boldsymbol{b}^*_{\alpha(s)\mu}$, $1 \leqq r < s \leqq p$, the two corresponding rhombus faces have the points

$$x_\mu = \tfrac{1}{2} \sum_{j=p+1}^{6} k_{\alpha(j)} \boldsymbol{b}^*_{\alpha(j)\mu} \pm y_\mu(\alpha(r), \alpha(s))$$
$$+ \tfrac{1}{2} (\lambda_{\alpha(r)} \boldsymbol{b}^*_{\alpha(r)\mu} + \lambda_{\alpha(s)} \boldsymbol{b}^*_{\alpha(s)\mu}) ,$$
$$y_\mu(\alpha(r), \alpha(s))$$
$$= \tfrac{1}{2} \sum_{i=1}^{p} \operatorname{sign}(\det(\boldsymbol{b}^*_{\alpha(i)\mu}, \boldsymbol{b}^*_{\alpha(r)\mu}, \boldsymbol{b}^*_{\alpha(s)\mu}))\, \boldsymbol{b}^*_{\alpha(i)\mu} .$$

Proof: This expression for the rhombus faces is derived in [3] under the general condition that any three different vectors in the set which spans the projected p-boundary are linearly independent. This property clearly holds in the present case.

The projection of the unit cell $k(6; \alpha, k)$ is the triacontahedron found by Kepler [4]. For $p = 5, 4, 3$ one finds the icosahedron, the dodecahedron and the two hexahedra described in [2] Section 7.

These polyhedra appear in the projection as the images of the p-boundaries of the unit cell. This means that they appear inside the triacontahedron which is the projection of the unit cell. To get a systematic enumeration of the possible position of a projected p-boundary inside the projected unit cell, one can apply the orbit analysis of Section 3 and specify for each orbit a single representative. These representatives for the projection $\mathbb{E}^6$ to $\mathbb{E}^3_1$ are displayed in Figs. 1–6. In these figures, the representatives are shown in projections of the triacontahedron along one or two orthogonal 2-fold rotation axes. The representatives are identified by their centers and denoted according to Table 1.

The full projection of the unit cell and of all its boundaries clearly is an object of considerable complexity. The 64 vertices for example appear in the form of the 32 outer vertices of the triacontahedron and 32 inner vertices. There are 60 outer and

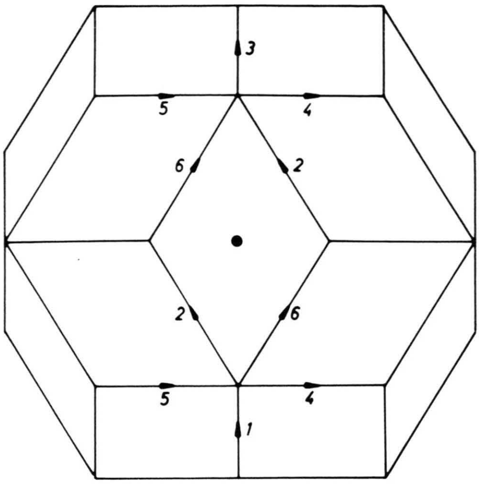

Fig. 1. The triacontahedron in $\mathbb{E}^3_1$ is the projection of the hypercubic unit cell from $\mathbb{E}^6$. The triacontahedron is shown in parallel projection along a 2-fold axis. The projections of the six basis vectors from $\mathbb{E}^6$ to $\mathbb{E}^3_1$ form the edges of the triacontahedron. Their directions are marked by arrows and by the numbers 1, ..., 6.

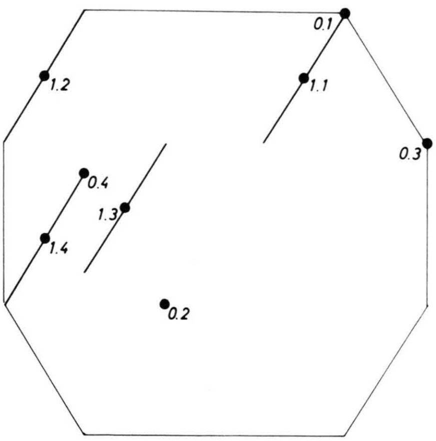

Fig. 2. Representatives of 0-boundaries marked 0.1, ..., 0.4 and of 1-boundaries marked 1.1, ..., 1.4 in the projection from $\mathbb{E}^6$ to $\mathbb{E}^3_1$. The centers of the projections are marked by circles. All points and lines are in a plane through the center of the triacontahedron perpendicular to the direction of the projection.

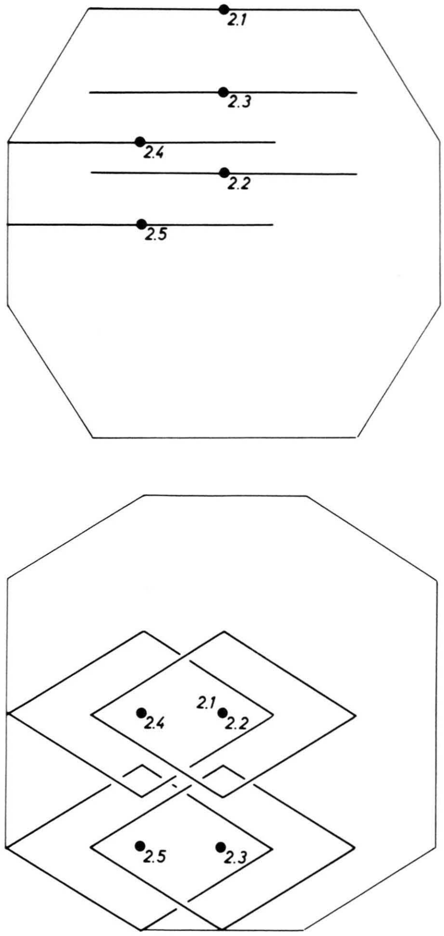

Fig. 3. Representatives of 2-boundaries marked 2.1, ..., 2.5 in the projection from $\mathbb{E}^6$ to $\mathbb{E}^3_1$. They are shown in parallel projections along two 2-fold axes orthogonal to one another.

132 inner 1-boundaries, 30 outer and 210 inner 2-boundaries. These boundaries as well as the 3-, 4-, and 5-boundaries will play an important part in the analysis of the quasilattice which will be developed in Sections 6–9.

As was discussed in Section 3, the p-boundaries in the full hypercubic lattice have additional point symmetry groups with respect to their centers. These point groups are generated by the space group and isomorphic to subgroups $\Omega(p) \times \Omega(6-p)$ of the point group $\Omega(6)$. If $\Omega(6)$ is now restricted to its subgroup $A(5)$, these point groups are restricted to intersections of the type

$$H = (\Omega(p) \times \Omega(6-p)) \cap A(5)$$

and their conjugates. These intersections are isomorphic for p-boundaries on the same orbit under $A(5)$ and are found to be $A(5)$ itself or one of the dihedral subgroups $D(5)$, $D(2)$ or $D(3)$. They are included in Table 1.

In a similar fashion we can determine the projection of the first unit cell and its boundaries from

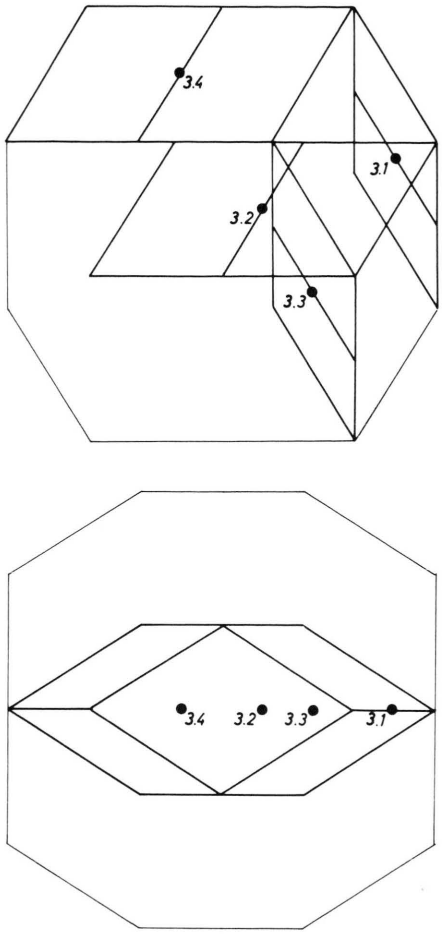

Fig. 4. Representatives of 3-boundaries marked 3.1, ..., 3.4 in two parallel projections along 2-fold axes. 3.1 and 3.3 are thin, 3.2 and 3.4 thick rhombohedra.

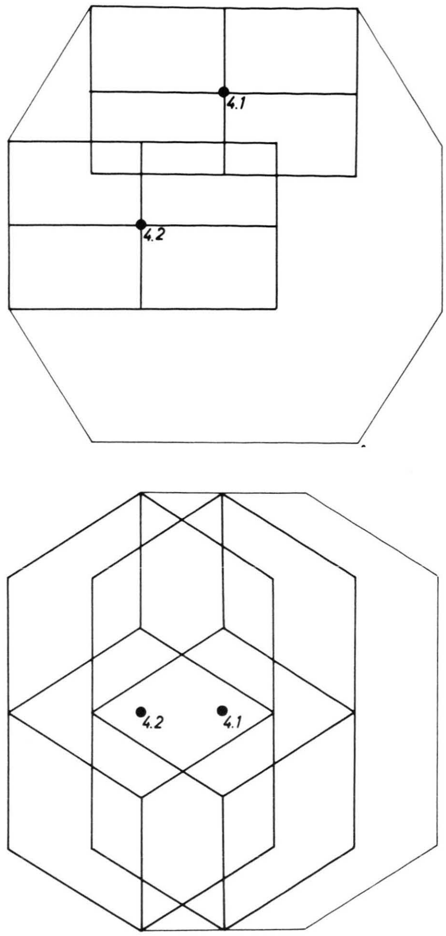

Fig. 5. Representatives of 4-boundaries marked 4.1, 4.2 in two parallel projections along 2-fold axes. The representatives are dodecahedra of the same shape with rhombus faces.

$\mathbb{E}^6$ to $\mathbb{E}_2^3$. To simplify the analysis we may connect the spaces $\mathbb{E}_1^3$ and $\mathbb{E}_2^3$ by the replacement

$$b_{i1}^* \to \varepsilon_i b_{f(i)2}^*,$$

where ε_i and $f(i)$ are given by

$$g_4^{-1} = \left| \begin{matrix} 1 & 2 & 3 & 4 & 5 & 6 \\ 1 & 3 & 5 & 2 & 4 & -6 \end{matrix} \right|,$$

compare Sect. 2 of [2].

Figures 1–6 are appropriate for $\mathbb{E}_1^3$. If the centers of the representatives are constructed in $\mathbb{E}_2^3$, these points appear in positions different from the ones marked in these figures. For example the point

$$x = -\tfrac{1}{2} \sum_{i=1}^{6} b_i^*$$

from the orbit 0.1 would appear in $\mathbb{E}_2^3$ at the position

$$x_2 = -\tfrac{1}{2} \sum_{i=1}^{6} b_{i2}^*.$$

With the replacement given above this point appears in the position marked 0.2 in Figure 2. So the vertices which appear in $\mathbb{E}_1^3$ on the boundary of the triacontahedron will appear in $\mathbb{E}_2^3$ on interior points.

6. Intersection and dualization in $\mathbb{E}^6$

We consider now the intersection of the lattice Y with a subspace $\mathbb{E}_1^3$ determined by an irreducible representation of the icosahedral group. The analysis

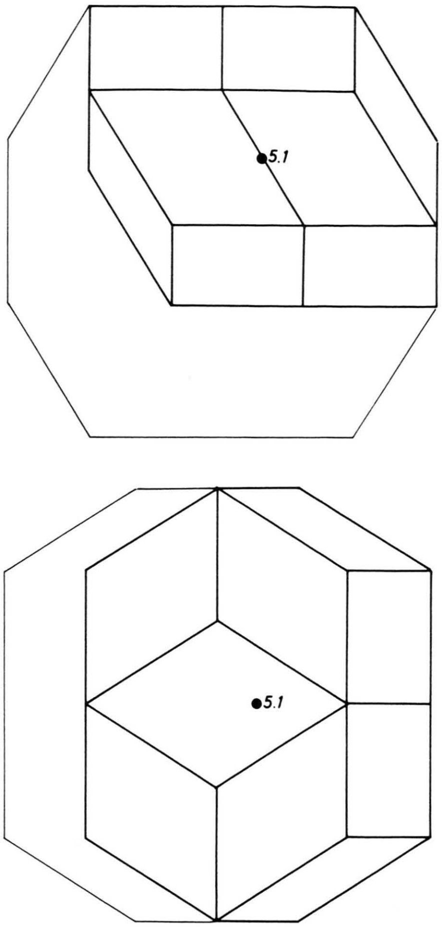

Fig. 6. Representative of 5-boundaries marked 5.1 in two parallel projections along 2-fold axes. The representative is an icosahedron with rhombus faces.

will be given in $\mathbb{E}^6$, and it will involve dualization between the lattices Y and Y^* of standard type. By the condition of intersection, we shall select in $\mathbb{E}^6$ a part of the dual lattice Y^* which we shall call a quasilattice Z in $\mathbb{E}^6$. This quasilattice will then be projected from $\mathbb{E}^6$ to $\mathbb{E}_1^3$. Its projection Z_1 will be shown to be essentially identical to the quasilattice Z_1 constructed in a different fashion in [2].

Throughout this section, γ is a fixed vector from the first unit cell of Y in $\mathbb{E}^6$, and hence γ obeys $-\frac{1}{2} \leqq \gamma \cdot \boldsymbol{b}_i \leqq \frac{1}{2}$, $i = 1, \ldots, 6$.

6.1. Definition: The first unit cell $\mathscr{h}\,(6; 1, \ldots, 6)$ has an intersection with $\mathbb{E}_1^3$ if there is a point

$$\boldsymbol{x}_1: -\tfrac{1}{2} \leqq (\boldsymbol{x}_1 + \gamma) \cdot \boldsymbol{b}_i \leqq \tfrac{1}{2}, \quad i = 1, \ldots, 6, \quad \boldsymbol{x}_1 \in \mathbb{E}_1^3 .$$

We extend this definition to p-boundaries of the first unit cell.

6.2. Definition: The p-boundary $\mathscr{h}\,(p; \alpha, k)$, $0 \leqq p \leqq 6$ has an intersection with $\mathbb{E}_1^3$ if there is a point

$$\boldsymbol{y} = \boldsymbol{x}_1 + \gamma, \quad \boldsymbol{x}_1 \in \mathbb{E}_1^3$$

which belongs to $\mathscr{h}\,(p; \alpha, k)$ and hence obeys

$$-\tfrac{1}{2} \leqq \boldsymbol{y} \cdot \boldsymbol{b}_{\alpha(i)} \leqq \tfrac{1}{2}, \quad i = 1, \ldots, p;$$
$$\boldsymbol{y} \cdot \boldsymbol{b}_{\alpha(j)} = \tfrac{1}{2} k_{\alpha(j)}, \quad j = p+1, \ldots, 6 .$$

The intersection is called interior if the strict inequalities hold for $i = 1, \ldots, p$, that is, if the intersection involves an interior point of $\mathscr{h}\,(p; \alpha, k)$.

With respect to interior intersections we observe the following properties: Suppose that a p-boundary $\mathscr{h}(p)$ has an intersection with $\mathbb{E}_1^3$ which is not interior. Then there is a p'-boundary $\mathscr{h}\,(p')$, $p' < p$ of $\mathscr{h}\,(p)$ which has an interior intersection with $\mathbb{E}_1^3$, or else $\mathscr{h}\,(p)$ has a 0-boundary (0) which intersects with $\mathbb{E}_1^3$. Conversely suppose that $\mathscr{h}\,(p')$ has an interior intersection with $\mathbb{E}_1^3$. Then all p-boundaries $\mathscr{h}\,(p)$ for $p = p' + 1, \ldots, 6$ which have $\mathscr{h}(p')$ as a boundary necessarily have a non-interior intersection with $\mathbb{E}_1^3$.

The equations and inequalities occurring in Def. 6.1 and 6.2 are, up to certain equality signs, identical to the conditions specified for the hexagrid Y_1 described in Sect. 3 of [2]. The difference is in the interpretation since here we stress the geometric objects found in $\mathbb{E}^6$ whereas the hexagrid description was given in $\mathbb{E}_1^3$.

6.3. Proposition: The p-boundaries of the first unit cell in $\mathbb{E}^6$ which intersect with $\mathbb{E}_1^3$ are in one-to-one correspondence to intersections of $(6 - p)$ planes which form the boundaries of the first cell of the hexagrid Y_1 in $\mathbb{E}_1^3$. In particular, the 5-boundaries correspond to the plane faces of this hexagrid cell.

So the hexagrid description can be seen as a very convenient way of representing the intersection of the 6-dimensional lattice Y with the 3-dimensional space $\mathbb{E}_1^3$. The equivalent interpretation in $\mathbb{E}^6$ according to Defs. 6.1 and 6.2 will play a key role in the new definition of the quasilattice to which we turn next.

6.4. Definition: Suppose that the p-boundary $\mathscr{h}(p; \alpha, k)$, $1 \leqq p \leqq 6$, of the first unit cell has an interior intersection with $\mathbb{E}_1^3$. Then its dual $\mathscr{h}^*\,(6 - p; \alpha, k)$ is defined as part of a quasilattice Z in $\mathbb{E}^6$. By extending this definition to all cells of Y

which intersect with $\mathbb{E}_1^3$, the quasilattice Z in $\mathbb{E}^6$ is defined as a part of the dual lattice Y^*. For $p=0$, the dual $\mathscr{h}^*(6)$ is included into the quasilattice Z if $\mathscr{h}(0)$ intersects with $\mathbb{E}_1^3$.

This definition employs the standard concept of dualization in $\mathbb{E}^n$ described in Sect. 2 of the present paper. No new type of dualization will be required in the approach followed here.

Consider now in detail the construction of the quasilattice Z according to Definition 6.4. Since the first unit cell of Y, denoted by $\mathscr{h}(6; 1, \ldots, n)$, has an intersection with $\mathbb{E}_1^3$, the quasilattice Z has a first vertex or 0-boundary $z=0$.

Any interior intersection with a 5-boundary of Y determines a 1-boundary of Z, that is, a line segment going out from the point $z=0$ in the direction of a vector $\boldsymbol{b}_{\alpha(6)}$. In general, all p-boundaries of Y intersecting with $\mathbb{E}_1^3$ give rise to dual $(6-p)$-boundaries of Z which have the 0-boundary $z=0$ as an intersection.

The extension of the quasilattice Z beyond the duals of the first unit cell follows with the help of Proposition 2.6. Since a 5-boundary of Y is always shared by two neighbouring unit cells, the 5-boundaries which have an intersection with $\mathbb{E}_1^3$ determine the steps to the next cells which have intersections with $\mathbb{E}_1^3$. In terms of the quasilattice Z, the dual 0-boundaries to these cells are the endpoints of the vectors $\boldsymbol{b}_{\alpha(6)}$ starting at $z=0$. The construction of Z may then be continued from these new points.

We have described in $\mathbb{E}^6$ a quasilattice Z consisting of selected parts from the dual lattice Y^*. Now we project this quasilattice Z down to the subspace $\mathbb{E}_1^3$. In $\mathbb{E}_1^3$, the initial vertex becomes the point

$$z_1 = 0$$

and the 1-boundaries going from this point are in the direction of the vectors $\boldsymbol{b}_{\alpha(6)1}$.

This construction of the projected quasilattice resembles the construction of the quasilattice Z_1 discussed in Sect. 4 of [2]. In [2], the quasilattice Z_1 was obtained by a different type of "dualization" which leads from the hexagrid Y_1 to the quasilattice Z_1. We consider it as a great advantage of the present approach that this different type of dualization can be avoided by carrying out the analysis in the original space $\mathbb{E}^6$.

6.5. Definition: The quasilattice Z_1 in $\mathbb{E}_1^3$ is the projection of the quasilattice Z from $\mathbb{E}^6$ to $\mathbb{E}_1^3$.

A comparison of this new definition with the old prescription for Z_1 given in Sect. 4 of [2] shows the following differences: In [2] the first vertex of the quasilattice was the point

$$v_1 = \tfrac{1}{2} \sum_{i=1}^{6} \boldsymbol{b}_{i1},$$

whereas now it is the point $z_1 = 0$. The dual parts of p-boundaries from Y for $p = 5, 4, 3$ project into edges, faces and rhombohedra which intersect in the first vertex. A conceptual difference occurs for p-boundaries of Y with $p = 2, 1, 0$. The dual parts of Z are of dimension $6-p = 4, 5, 6$ and under projection to $\mathbb{E}_1^3$ become the composite cells described in Sect. 7 of [2] and in Sect. 5 of the present paper. In the hexagrid approach, these composite cells are obtained by "dualization" of a local intersection of $6-p$ planes in the hexagrid. In the present approach, they are projections of $(6-p)$-dimensional polytopes and inherit from these polytopes the projections of all their boundaries. We summarize this analysis.

6.6. Proposition: Given a hypercubic lattice in $\mathbb{E}^6$, its dual Y^*, a fixed point γ from the first unit cell of Y and the subspace $\mathbb{E}_1^3$ of $\mathbb{E}^6$, one can determine the p-boundaries of Y which have interior intersections with $\mathbb{E}_1^3$. The $(6-p)$-boundaries of Y^* dual to these intersecting p-boundaries form a quasilattice Z in $\mathbb{E}^6$. The projection of this quasilattice from $\mathbb{E}^6$ to $\mathbb{E}_1^3$ yields, up to shift of origin and the internal structure of the composite cells, the 3-dimensional quasilattice Z_1 constructed in a different way in [2].

7. Kepler Zone Structure and the γ-Diagnosis for the Quasilattice

The six-dimensional approach to the quasilattice developed in the preceding sections opens up a completely new way to a description of the quasilattice which will be developed in this and the following section.

7.1. Proposition. The p-boundary $\mathscr{h}(p; \alpha, k)$ of the first unit cell in Y has an interior intersection with $\mathbb{E}_1^3$ if and only if the point $\gamma_2 \in \mathbb{E}_2^3$ is the projection of an interior point of this boundary from $\mathbb{E}^6$ to $\mathbb{E}_2^3$.

Proof: Decompose the vector γ as

$$\gamma = \gamma_1 + \gamma_2$$

and assume an interior intersection of the p-boundary $\mathscr{k}\,(p;\alpha,k)$ with $\mathbb{E}_1^3$. Then according to Def. 6.2 there is a point $x_1 \in \mathbb{E}_1^3$ such that

$$-\tfrac{1}{2} < (x_1 + y_1 + y_2) \cdot b_{\alpha(i)} < \tfrac{1}{2}, \quad i = 1, \ldots, p,$$
$$(x_1 + y_1 + y_2) \cdot b_{\alpha(j)} = \tfrac{1}{2} k_{\alpha(j)}, \quad j = p+1, \ldots, 6.$$

Clearly then y_2 is the projection to $\mathbb{E}_2^3$ of the point $(x_1 + y_1 + y_2)$ from $\mathscr{k}\,(p;\alpha,k)$. Conversely assume that there is a point $u_1 \in \mathbb{E}_1^3$ such that $u_1 + y_2$ is a point from $\mathscr{k}(p;\alpha,k)$. Define

$$x_1 = u_1 - y_1$$

to find that the point x_1 determines an interior intersection of $\mathscr{k}(p;\alpha,k)$ with $\mathbb{E}_1^3$.

To use Prop. 7.1 for the analysis of the first cell of the quasilattice, it is of great importance to have a criterion for the case that a point x_2 is the projection of an interior point from a p-boundary. For $p = 4, 5, 6$ this is not trivial since, in the projections of these cells to $\mathbb{E}_2^3$, the projections from the boundary points in $\mathbb{E}^6$ overlap with projections from interior points in $\mathbb{E}^6$. We must distinguish between the projections $\mathscr{k}_2(p)$ of p-boundaries from $\mathbb{E}^6$ and the boundaries of the projections which we denote as $s\mathscr{k}_2(p)$. The latter boundaries are the rhombus faces, their edges and vertices which characterize the projections. Now we claim and prove in Appendix A.

7.2. Proposition: A point x_2 is the projection of an interior point x of a p-boundary $\mathscr{k}\,(p)$ to $\mathbb{E}_2^3$ if and only if it is an interior point of $\mathscr{k}_2(p)$, the projection of $\mathscr{k}\,(p)$ to $\mathbb{E}_2^3$, that is, if $x_2 \in \mathscr{k}_2(p)$ but $x_2 \notin s\mathscr{k}_2(p)$.

Note that we include the possibility that the point x_2, which is the projection of an interior point of $\mathscr{k}\,(p)$, is at the same time the projection of a point from a boundary of $\mathscr{k}\,(p)$.

Now we implement Prop. 7.1 for the analysis of the intersection of the lattice Y with $\mathbb{E}_1^3$.

7.3. Definition: The Kepler zone is the projection of the first unit cell of Y and of all its p-boundaries, $0 \leqq p \leqq 6$ from $\mathbb{E}^6$ to $\mathbb{E}_2^3$.

According to Sect. 5, this projection has the form of the triacontahedron introduced by Kepler in relation to his crystallographic ideas [4] and his concept of congruence [5]. The relation of Kepler's ideas to a hypercube in six dimensions has been developed by Kowalewski [6]. Whereas in Sect. 5 we considered the projection of the unit cell from $\mathbb{E}^6$ to $\mathbb{E}_1^3$, we require here the projection to $\mathbb{E}_2^3$. Fortunately these two projections are closely related. If in $\mathbb{E}^3$ we replace the projections of the basis vectors b_{i1} by the projections b_{i2} according to Section 5, we can transcribe all of the analysis given in Sect. 5 for $\mathbb{E}_1^3$ into a corresponding analysis for $\mathbb{E}_2^3$.

7.4. Proposition: The p-boundaries of the first unit cell of Y which intersect with $\mathbb{E}_1^3$ are completely specified by the position of the point y_2 in the Kepler zone. The p-boundary $\mathscr{k}\,(p;\alpha,k)$ has an interior intersection with $\mathbb{E}_1^3$ if and only if its projection inside the Kepler zone contains the interior point y_2. The point y_2 is restricted to the interior of the Kepler zone.

Note that the projections of the p-boundaries overlap in many ways inside the Kepler zone, as indicated in Section 5. The full orbit analysis given there is required to identify the various projections. We observe the following characteristics of the analysis: A given point y_2 always belongs to several (precisely to at least four) projections of 5-boundaries. It also belongs to projections of 4- and 3-boundaries. The projections of 2-, 1-, and 0-boundaries occur in the form of a rhombus, a line or a point in the Kepler zone. As long as y_2 is not a point from one of these latter boundaries, there are intersections at most with 5-, 4-, and 3-boundaries.

It is possible to pass from the diagnosis of a point y_2 in the Kepler zone of $\mathbb{E}_2^3$ directly to the corresponding vertex of the quasilattices Z or Z_1. At the vertex $z = 0$, it is simply necessary to construct the 1-boundaries dual to the 5-boundaries for which y_2 is the projection of an interior point. This construction extends to dual 2- and 3-boundaries which appear in Z_1 as rhombus faces and rhombohedra. If y_2 happens to be a projection of an interior point from a 2-, 1-, or from a 0-boundary, the boundaries of dimension 4, 5, 6 appear in the quasilattice Z and their projections appear as composite cells in Z_1, all of them with the common vertex $z = 0$ or $z_1 = 0$ respectively. So the diagnosis of the point y_2 in the Kepler zone yields the complete description of the quasilattice Z_1 at an initial vertex. An example will be discussed in Section 9.

Here we analyze a case which is of particular importance for the space filling property of the quasilattice Z_1. Consider a point y_2 which is the projection of a 4-boundary. These projections occur in the form of dodecahedra inside the Kepler zone in positions indicated in Figure 6. A 4-boundary has 3-boundaries which in the projection to $\mathbb{E}_2^3$ appear as 4 rhombohedra inside the dodecahedron. If y_2 is a point from the dodecahedron, which does not belong to one of its boundaries of dimension 0, 1, 2, it can easily be shown that it will belong to two overlapping rhombohedra which share an outer face of the dodecahedron.

As an example we consider the 4-boundary spanned by the vectors $\boldsymbol{b}_1, \boldsymbol{b}_2, \boldsymbol{b}_4, \boldsymbol{b}_5$. For simplicity we indicate the projections to $\mathbb{E}_1^3$ and $\mathbb{E}_2^3$ by the subindex 1, 2 to sums of vectors. A possible projection to the Kepler zone is

$$\hbar_2(4):\ \boldsymbol{x}_2 = \tfrac{1}{2}(\boldsymbol{b}_3^* + \boldsymbol{b}_6^*)_2 + \tfrac{1}{2}(\lambda_1 \boldsymbol{b}_1^* + \lambda_2 \boldsymbol{b}_2^* + \lambda_4 \boldsymbol{b}_4^* + \lambda_5 \boldsymbol{b}_5^*)_2 .$$

Three typical pairs of overlapping 3-boundaries $\hbar_2'(3)$, $\hbar_2''(3)$ which intersect in an outer rhombus face $\hbar_2(2)$ of $\hbar_2(4)$ are

I: Two thick rhombohedra

$\hbar_2'(3)$:
$$\boldsymbol{x}_2 = \tfrac{1}{2}(\boldsymbol{b}_3^* + \boldsymbol{b}_6^* + \boldsymbol{b}_2^*)_2 + \tfrac{1}{2}(\lambda_1 \boldsymbol{b}_1^* + \lambda_4 \boldsymbol{b}_4^* + \lambda_5 \boldsymbol{b}_5^*)_2 ,$$

$\hbar_2''(3)$:
$$\boldsymbol{x}_2 = \tfrac{1}{2}(\boldsymbol{b}_3^* + \boldsymbol{b}_6^* + \boldsymbol{b}_4^*)_2 + \tfrac{1}{2}(\lambda_1 \boldsymbol{b}_1^* + \lambda_2 \boldsymbol{b}_2^* + \lambda_5 \boldsymbol{b}_5^*)_2 ,$$

$\hbar_2(2)$:
$$\boldsymbol{x}_2 = \tfrac{1}{2}(\boldsymbol{b}_3^* + \boldsymbol{b}_6^* + \boldsymbol{b}_2^* + \boldsymbol{b}_4^*)_2 + \tfrac{1}{2}(\lambda_1 \boldsymbol{b}_1^* + \lambda_5 \boldsymbol{b}_5^*)_2 .$$

II: Two thin rhombohedra

$\hbar_2'(3)$:
$$\boldsymbol{x}_2 = \tfrac{1}{2}(\boldsymbol{b}_3^* + \boldsymbol{b}_6^* + \boldsymbol{b}_5^*)_2 + \tfrac{1}{2}(\lambda_1 \boldsymbol{b}_1^* + \lambda_2 \boldsymbol{b}_2^* + \lambda_4 \boldsymbol{b}_4^*)_2 ,$$

$\hbar_2''(3)$:
$$\boldsymbol{x}_2 = \tfrac{1}{2}(\boldsymbol{b}_3^* + \boldsymbol{b}_6^* + \boldsymbol{b}_1^*)_2 + \tfrac{1}{2}(\lambda_2 \boldsymbol{b}_2^* + \lambda_4 \boldsymbol{b}_4^* + \lambda_5 \boldsymbol{b}_5^*)_2 ,$$

$\hbar_2(2)$:
$$\boldsymbol{x}_2 = \tfrac{1}{2}(\boldsymbol{b}_3^* + \boldsymbol{b}_6^* + \boldsymbol{b}_1^* + \boldsymbol{b}_5^*)_2 + \tfrac{1}{2}(\lambda_2 \boldsymbol{b}_2^* + \lambda_4 \boldsymbol{b}_4^*)_2 .$$

III. A thick and a thin rhombohedron

$\hbar_2'(3)$:
$$\boldsymbol{x}_2 = \tfrac{1}{2}(\boldsymbol{b}_3^* + \boldsymbol{b}_6^* + \boldsymbol{b}_2^*)_2 + \tfrac{1}{2}(\lambda_1 \boldsymbol{b}_1^* + \lambda_4 \boldsymbol{b}_4^* + \lambda_5 \boldsymbol{b}_5^*)_2 ,$$

$\hbar_2''(3)$:
$$\boldsymbol{x}_2 = \tfrac{1}{2}(\boldsymbol{b}_3^* + \boldsymbol{b}_6^* + \boldsymbol{b}_5^*)_2 + \tfrac{1}{2}(\lambda_1 \boldsymbol{b}_1^* + \lambda_2 \boldsymbol{b}_2^* + \lambda_4 \boldsymbol{b}_4^*)_2 ,$$

$\hbar_2(2)$:
$$\boldsymbol{x}_2 = \tfrac{1}{2}(\boldsymbol{b}_3^* + \boldsymbol{b}_6^* + \boldsymbol{b}_2^* + \boldsymbol{b}_5^*)_2 + \tfrac{1}{2}(\lambda_1 \boldsymbol{b}_1^* + \lambda_4 \boldsymbol{b}_4^*)_2 .$$

In the quasilattice Z_1, the dual 3-boundaries appear in pairs which have the 2-boundary dual to the 4-boundary $\hbar(4)$ in common. This 2-boundary is given by

$$\hbar_1(2):\ \boldsymbol{x}_1 = \tfrac{1}{2}(\boldsymbol{b}_3 + \boldsymbol{b}_6)_1 + \tfrac{1}{2}(\lambda_3 \boldsymbol{b}_3 + \lambda_6 \boldsymbol{b}_6)_1 .$$

The pairs of rhombohedra have the description

I: Two thick rhombohedra

$\hbar_1'(3)$:
$$\boldsymbol{x}_1 = \tfrac{1}{2}((1+\lambda_3)\,\boldsymbol{b}_3 + (1+\lambda_6)\,\boldsymbol{b}_6 + (1+\lambda_2)\,\boldsymbol{b}_2)_1 ,$$

$\hbar_1''(3)$:
$$\boldsymbol{x}_1 = \tfrac{1}{2}((1+\lambda_3)\,\boldsymbol{b}_3 + (1+\lambda_6)\,\boldsymbol{b}_6 + (1+\lambda_4)\,\boldsymbol{b}_4)_1 .$$

II. Two thin rhombohedra

$\hbar_1'(3)$:
$$\boldsymbol{x}_1 = \tfrac{1}{2}((1+\lambda_3)\,\boldsymbol{b}_3 + (1+\lambda_6)\,\boldsymbol{b}_6 + (1+\lambda_5)\,\boldsymbol{b}_5)_1 ,$$

$\hbar_1''(3)$:
$$\boldsymbol{x}_1 = \tfrac{1}{2}((1+\lambda_3)\,\boldsymbol{b}_3 + (1+\lambda_6)\,\boldsymbol{b}_6 + (1+\lambda_1)\,\boldsymbol{b}_1)_1 .$$

III. A thick and a thin rhombohedron

$\hbar_1'(3)$:
$$\boldsymbol{x}_1 = \tfrac{1}{2}((1+\lambda_3)\,\boldsymbol{b}_3 + (1+\lambda_6)\,\boldsymbol{b}_6 + (1+\lambda_2)\,\boldsymbol{b}_2)_1 ,$$

$\hbar_1''(3)$:
$$\boldsymbol{x}_1 = \tfrac{1}{2}((1+\lambda_3)\,\boldsymbol{b}_3 + (1+\lambda_6)\,\boldsymbol{b}_6 + (1+\lambda_5)\,\boldsymbol{b}_5)_1 .$$

For a given pair, the two rhombohedra have only the face $\hbar_1(2)$ in common. The positions of the 3-boundaries in the Kepler zone and in the quasilattice are shown in the left and right parts respec-

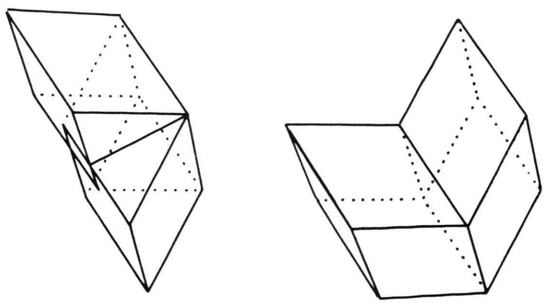

Fig. 7. *Left:* Two thick rhombohedra in the Kepler zone which overlap and share a face. *Right:* The duals to these rhombohedra in the quasilattice are two thick rhombohedra which share only a face.

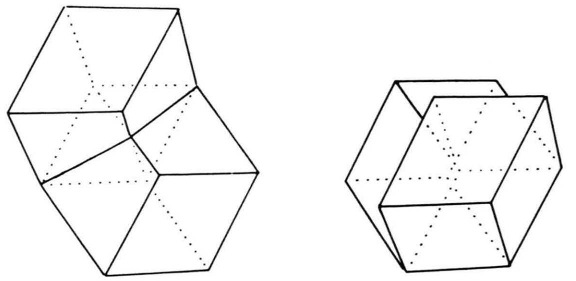

Fig. 8. *Left:* Two thin rhombohedra in the Kepler zone which overlap and share a face. *Right:* The duals in the quasilattice are two thin rhombohedra which share only a face.

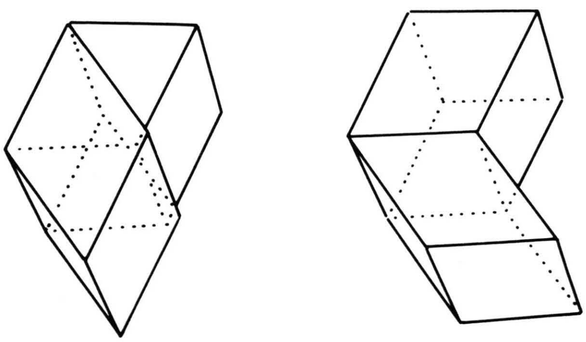

Fig. 9. *Left:* A thin and a thick rhombohedron in the Kepler zone which overlap and share a face. *Right:* The duals in the quasilattice are similar rhombohedra which share only a face.

tively of Figures 7, 8, 9. The orientation in $\mathbb{E}^3$ has been chosen in these figures so that the position of the rhombohedra can easily be recognized.

A systematic exhaustive classification shows that these three typical cases cover, up to shifts and icosahedral rotations, all the relative positions of rhombohedra in the quasilattice. From this we infer the matching rule that two rhombohedra with a common face and the same shape can never occur in positions related by a parallel shift.

8. The Graph of the Quasilattice

In Sect. 7 it was shown that the location of the vector γ_2 in the Kepler zone allows for a complete diagnosis of all boundaries and their duals of the lattice Y and the quasilattice Z. Now we show how this analysis may be extended to the full quasilattice.

Suppose that the initial vector γ_2 is the projection of an interior point from a fixed 5-boundary shared by the first unit cell of the lattice Y and a neighbouring cell centered at

$$\boldsymbol{u} = k_{\alpha(6)}\, \boldsymbol{b}^*_{\alpha(6)} .$$

This implies that

$$\gamma' = \gamma - \boldsymbol{u}$$

is a vector from the first unit cell and hence

$$\gamma_2' = \gamma_2 - \boldsymbol{u}_2$$

is a new point from the Kepler zone. This new point γ_2' may be analyzed by the methods of Sect. 7 with respect to its position as a projection of p-boundaries. The duals to these p-boundaries determine new parts of the quasilattice Z whose centers must then be shifted back by the vector

$$\boldsymbol{u} = k_{\alpha(6)}\, \boldsymbol{b}_{\alpha(6)}$$

in $\mathbb{E}^6$ for the quasilattice Z, and by the vector

$$\boldsymbol{u}_1 = k_{\alpha(6)}\, \boldsymbol{b}_{\alpha(6)1}$$

in $\mathbb{E}^3_1$ for the quasilattice Z_1.

To display the connection of γ_2 and γ_2' we draw the edge with points

$$\boldsymbol{w}_2 = \gamma_2 - \tfrac{1}{2}\,(\lambda_{\alpha(6)} + k_{\alpha(6)})\, \boldsymbol{b}^*_{\alpha(6)2}$$

which connects γ_2 and γ_2'. The application to all other 5-boundaries and the subsequent continuation from γ_2' to γ_2'', ... yields a graph K for the quasilattice whose vertices are all inside the Kepler zone.

Note that the assumed 5-boundary in Z_1 gives rise to the edge line

$$z_1 = \tfrac{1}{2}\,(\lambda_{\alpha(6)} + k_{\alpha(6)})\, \boldsymbol{b}_{\alpha(6)1} .$$

Therefore there is a complete correspondence between the vertices and edge lines of the graph K described above and the vertices and edge lines of the quasilattice Z_1. Each vertex could be indexed by a set of six integers which describe the integer linear combinations of the basis vectors by which it is reached from some initial vertex:

To the vertex

$$z_1(n_1, \ldots, n_6) = \sum_{i=1}^{6} n_i \boldsymbol{b}_{i1}$$

of the quasilattice Z_1 there corresponds the vertex

$$\gamma_2(n_1, \ldots, n_6) = \gamma_2(0, \ldots, 0) - \sum_{i=1}^{6} n_i b_{i2}^*$$

of the graph K.

8.1. Proposition: The initial point γ_2 in the Kepler zone determines an infinite connected graph K inside the Kepler zone. This graph K gives a complete description of the infinite quasilattice Z_1. There is a one-to-one correspondence between the vertices and edges of K and Z_1.

9. An example for a graph of a quasilattice

To illustrate some aspects of the description of a quasilattice by its graph K we discuss here a specific example. We shall make use of the projection of the first unit cell of the lattice from $\mathbb{E}^6$ to $\mathbb{E}_2^3$.

As the initial point in the Kepler zone we choose

$$\gamma_2 = -\tfrac{1}{2} \sum_{j=1}^{6} b_{j2}^* .$$

This point is the projection of a 0-boundary and, in the orbit analysis applied to $\mathbb{E}_2^3$, corresponds to the representative marked 0.2 shown in Figure 2. We discuss now the other p-boundaries which have γ_2 as their projection. These boundaries may be indexed by the numbers $(k_1 k_2 k_3 k_4 k_5 k_6)$ according to Defs. 2.2 and 2.4.

In Table 2 we give the six 5-boundaries to which γ_2 belongs, the dual vertices of the quasilattice Z, and the new points γ_2' which can be reached from γ_2 in the graph K. Note that the point γ_2 belongs to the 5-boundary $(00000\bar{1})$ but is a point on its boundary $s\mathscr{h}_2(5)$. Hence this boundary is not listed in Table 2.

Comparing the positions of 2-boundaries from Table 1 and Fig. 3, one finds that γ_2 is the projection of an interior point of the 2-boundaries with index systems

$(\bar{1}0101\bar{1}1)$
$(\bar{1}\bar{1}0101)$
$(0\bar{1}\bar{1}011)$
$(10\bar{1}\bar{1}01)$
$(010\bar{1}\bar{1}1)$

The cells around the first vertex of the quasilattice Z_1 located at $z_1 = 0$ are then a projected 6-boundary or triacontahedron dual to the 0-boundary with its center at $(\bar{1}\bar{1}\bar{1}\bar{1}\bar{1}\bar{1})$, and five projected 4-boundaries or dodecahedra dual to the 2-boundaries listed above.

As an example of the continuation of the graph K we choose from Table 2

$$\gamma_2' = \gamma_2 + b_{32}^* .$$

This point is again the projection of a 0-boundary and belongs to the orbit with representative 0.4 in Figure 2. In Table 3 we give the analysis corresponding to Table 2 for this point in the Kepler zone. Moreover γ_2' is found to be the projection of interior points from the 2-boundaries

$(1\bar{1}0\bar{1}10)$
$(0\bar{1}1011)$
$(101\bar{1}01)$

and from the 3-boundary

(100011)

Since γ_2' is also the projection of a 0-boundary, the cells around the new vertex of the quasilattice Z_1 located at $z_1 = -b_{31}$ are a triacontahedron, three dodecahedra and a thick rhombohedron. The center

Table 2. The 5-boundaries in the Kepler zone, the dual vertices of the quasilattice reached by the dual edge lines, and the new vertices γ_2' reached in the graph K from $\gamma_2 = -\frac{1}{2}\sum_j b_{j2}^*$.

5-boundary $(k_1 k_2 k_3 k_4 k_5 k_6)$	New vertex of Z_1	New vertex γ_2' of K
$(\bar{1}00000)$	$-b_{11}$	$\gamma_2 + b_{12}^*$
$(0\bar{1}0000)$	$-b_{21}$	$\gamma_2 + b_{22}^*$
$(00\bar{1}000)$	$-b_{31}$	$\gamma_2 + b_{32}^*$
$(000\bar{1}00)$	$-b_{41}$	$\gamma_2 + b_{42}^*$
$(0000\bar{1}0)$	$-b_{51}$	$\gamma_2 + b_{52}^*$
(000001)	b_{61}	$\gamma_2 - b_{62}^*$

Table 3. The 5-boundaries in the Kepler zone, the dual vertices of the quasilattice, and the new vertices γ_2'' reached in the graph K from $\gamma_2' = \gamma_2 + b_{32}^*$.

5-boundary $(k_1 k_2 k_3 k_4 k_5 k_6)$	New vertex of Z_1	New vertex γ_2'' of K
(001000)	b_{31}	$\gamma_2' - b_{32}^*$
$(000\bar{1}00)$	$-b_{41}$	$\gamma_2' + b_{42}^*$
$(0\bar{1}0000)$	$-b_{21}$	$\gamma_2' + b_{22}^*$
(100000)	b_{11}	$\gamma_2' - b_{12}^*$
(000010)	b_{51}	$\gamma_2' - b_{52}^*$
(000001)	b_{61}	$\gamma_2' - b_{61}^*$

of the triacontahedron is located at

$$x_1 = -b_{31} - \tfrac{1}{2}(b_{11} + b_{21} - b_{31} + b_{41} + b_{51} + b_{61})$$
$$= -\tfrac{1}{2}(b_{11} + b_{21} + b_{31} + b_{41} + b_{51} + b_{61})$$

and so it is identical with the one found also at the vertex $z_1 = 0$ corresponding to γ_2. Similarly, the second and third dodecahedron are identical to the third and fourth dodecahedron found at $z_1 = 0$.

Of the points γ_2'' which can be reached from γ_2', the first one is simply the old point γ_2. The second and third point are again projections of 0-boundaries and belong to the same orbit with representative 0.2 as γ_2.

The graph K can be continued by entirely analogous steps to encompass all projections of 0-boundaries which belong to the orbits 0.2 and 0.4 of Table 1. All these 32 points in the Kepler zone are pairwise linked by the graph K as shown in Figure 10. This part of the graph has already icosahedral point symmetry. The dual part of the quasilattice starts with a central triacontahedron surrounded by a layer of 30 dodecahedra. At the vertices of this triacontahedron with 3-fold symmetry there is a thick rhombohedron which shares faces with three dodecahedra and a vertex with the triacontahedron.

The graph K continues to a new set of points which are no longer projections of 0-boundaries. The last entry of Table 1

$$\gamma_2' = \gamma_2 - b_{62}^*$$

is an example of this new set. The corresponding edge of the graph of K is marked in Fig. 10 by a broken line. In the quasilattice, the new set of points of this type yields the cells belonging to the next layer.

In the hexagrid approach, the quasilattice Z_1 is obtained from the special case where six planes intersect in a single initial vertex. Clearly this case has global icosahedral point symmetry. There is another possibility of global icosahedral point symmetry for $\gamma_2 = 0$. In this case the first cell of the hexagrid is a dodecahedron, and in the quasilattice the first vertex is shared by 20 thick rhombohedra. The points on the boundary $s\hbar_2(6; 1 \ldots 6)$ of the Kepler zone are excluded since according to Prop. 7.2 they are not projections of interior points.

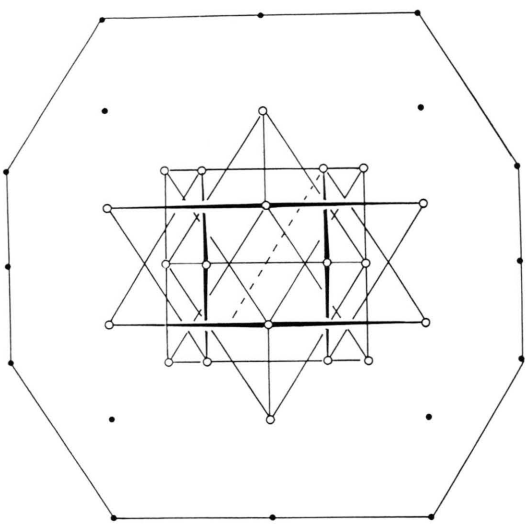

Fig. 10. Part of a graph K in the Kepler zone. The initial vertex is chosen in the position marked 0.2 in Figure 2. The graph K reaches all the 32 projections of 0-boundaries inside the Kepler zone, The edge lines are indicated by lines, and this part of the graph has already full icosahedral symmetry. The broken line is an edge line which leads to a new set of points. The full graph is infinite and non-periodic. To this graph there corresponds a quasilattice with icosahedral point symmetry. It contains a central triacontahedron whose faces are covered by 30 dodecahedra.

10. Global point symmetry

In view of the analysis presented in previous sections of this paper, the analysis of global point symmetry given in section 6 of [2] is not complete and requires extension. First of all it is necessary to admit for γ_2 all points from the Kepler zone, not only the points of the dodecahedron discussed in section 6 of [2]. The analysis of (6.6) of [2] remains valid if the range of the coefficients $\lambda_1, \lambda_4, \lambda_6$ is extended. We prefer to use the full Kepler zone as the region for the analysis of the point symmetry. Then the orbit analysis under A(5) given in Table 1 covers in principle the point symmetry for an initial point γ_2 in the Kepler zone.

In [2] it was indicated that the space group of the lattice in $\mathbb{E}^6$ yields additional point symmetries of the quasilattice. These point symmetries can now be identified with the help of the analysis given in Sects. 7 and 8 and in Table 1. In terms of the Kepler zone description, these new global point symmetries occur at the centers of the projected p-boundaries, compare Table 4.

Table 4. Global point symmetry group H of the quasilattice for points $\gamma_2 = \frac{1}{2} \sum_i k_i \boldsymbol{b}_{i2}^*$ of the Kepler zone which are projections of centers of p-boundaries.

p	H	$(k_1 k_2 k_3 k_4 k_5 k_6)$
0	A(5)	(111111)
6	A(5)	(000000)
1	D(5)	(111110)
5	D(5)	(000001)
2	D(2)	(111100)
4	D(2)	(000011)
3	D(3)	(111000)
3	D(3)	(000111)

11. General properties of the quasilattice

The graph K of a quasilattice Z_1 appears to be an important tool for the general analysis of structures in quasicrystallography. We discuss here some of these aspects.

First of all, the graph K is a global representation of the quasilattice Z_1 with no reference to a particular initial point. This means that quasilattices should be classified in terms of their graphs K. The classification in terms of a single initial vector γ_2 is insufficient.

The graph K offers a way of generating a quasilattice from an initial point. If an initial vector γ_2 is chosen, one can derive in a step-by-step procedure the next vertices $\gamma_2', \gamma_2'', \ldots$ and at the same time the vertices of the quasilattice Z_1. This procedure is completely deterministic and contains all the matching rules of the quasilattice. The analysis of Sect. 9 contains an example for this procedure.

The graph K contains the full information on the global point symmetry and on the appearance of local composite cells. A global point symmetry appears whenever one of the vertices γ_2 takes the special values discussed in Section 5. A local composite cell occurs whenever one of the vertices hits the projection of a 0-, 1-, or 2-boundary in the Kepler zone.

We turn now to the non-periodicity of the quasilattice and describe it in terms of the graph K. For this purpose we consider the function Γ_2 from the index system $(n_1, \ldots, n_6)$ to the vector γ_2 in the Kepler zone

$$\Gamma_2\colon\ (n_1, \ldots, n_6) \to \gamma_2(n_1, \ldots, n_6)\,,$$

$$\gamma_2(n_1, \ldots, n_6) = \gamma_2(0, \ldots, 0) - \sum_{i=1}^{6} n_i \boldsymbol{b}_{i2}^*\,.$$

It is clear that not all combinations of integers appear since not all cells of the lattice Y intersect with $\mathbb{E}_1^3$. We are of course free to choose any vertex of the graph K as initial point and to label it by the index system $(0, \ldots, 0)$. Then we have

11.1. Proposition: The graph K of the quasilattice Z_1 is non-periodic in terms of the function Γ_2, that is,

$$\gamma_2(m_1, \ldots, m_6) = \gamma_2(0, \ldots, 0)$$

implies $m_1 = \ldots = m_6 = 0$.

Proof: The equality of the vertices implies

$$\sum_{i=1}^{6} m_i \boldsymbol{b}_{i2}^* = 0$$

with the only solution $m_1 = \ldots = m_6 = 0$.

This result requires that the graph K stays in the Kepler zone but never returns to the same point. In the example of Sect. 9, the graph K can never return to the 32 points which yield a composite cell in the form of a triacontahedron.

Appendix A: Proof of Proposition 7.2

Proposition 7.2 states that for any interior point z_2 of a projected cell $\ell_2(p)$ in $\mathbb{E}_2^3$ for $p = 1, \ldots, 6$ and only for an interior point there exists an interior point z from (p) in $\mathbb{E}^6$ which has z_2 as its projection. We reduce the proposition to the form

A.1. Proposition: Let $\ell_2(p)$ be the convex cell

$$\ell_2(p) = \left\{ \boldsymbol{x}_2 \,\middle|\, \boldsymbol{x}_2 = \tfrac{1}{2} \sum_{i=1}^{p} \lambda_{\alpha(i)} \boldsymbol{b}_{\alpha(i)2}^*\,, \right.$$

$$\left. -1 \leqq \lambda_{\alpha(j)} \leqq 1, j = 1, \ldots, p \right\}.$$

If z_2 describes an interior point of $\ell_2(p)$, then the numbers $\lambda_{\alpha(j)}$ may be chosen in the interval

$$-1 < \lambda_{\alpha(j)} < 1\,,\quad j = 1, \ldots, p\,.$$

Once we have shown Prop. A.1, we can construct the vector

$$z = \tfrac{1}{2} \sum_{i=1}^{p} \lambda_{\alpha(i)} \boldsymbol{b}_{\alpha(i)}^*$$

in $\mathbb{E}^6$ which describes an interior point of the p-boundary $\ell(p)$ and has the projection z_2 to $\mathbb{E}_2^3$, and so we have shown proposition 7.2 for the interior points. For points z_2 on the boundary $s\,\mathscr{k}_2(p)$ of $\mathscr{k}_2(p)$ it is shown in Sect. A.5 of [3] that they uniquely determine points on the boundary of $\mathscr{k}\,(p)$ in $\mathbb{E}^6$. So proposition A.1 implies proposition 7.2. Now we reduce proposition A.1 to the form

A.2. Proposition. If z_2 describes an interior point of $\mathscr{k}_2(p), p = 2, \ldots, 6$, it may be written as

$$z_2 = y_2 + z_2',$$

where

$$y_2 = \tfrac{1}{2}\lambda_{\alpha(1)}\,\boldsymbol{b}^*_{\alpha(1)}, \quad -1 < \lambda_{\alpha(1)} < 1,$$

and where z_2' is an interior point, referred to the center, of the cell $\mathscr{k}_2(p-1)$ spanned by the vectors

$$\boldsymbol{b}^*_{\alpha(j)2}, \quad j = 2, \ldots, p.$$

This proposition is obviously true for $p = 2, 3$. If it is applied under the assumptions made in proposition A.1, any case $p = 4, 5, 6$ is reduced to a case $p-1$ where now the vector z_2' is an interior point of a cell $\mathscr{k}_2(p-1)$ and where the first number $\lambda_{\alpha(1)}$ has been fixed. So by reduction to $p = 3$ Prop. A.2 implies Prop. A.1 and hence Proposition 7.2.

Proof of Prop. A.2:

From the definition of $\mathscr{k}_2(p)$, a point may be written as

$$\boldsymbol{x}_2 = y_2 + \boldsymbol{x}_2', \qquad (*)$$

where

$$y_2 = \tfrac{1}{2}\lambda_{\alpha(1)}\,\boldsymbol{b}^*_{\alpha(1)2}, \quad -1 \leqq \lambda_{\alpha(1)} \leqq 1,$$

and where $\boldsymbol{x}_2'$ is a vector for a point of the cell $\mathscr{k}_2(p-1)$ spanned by the vectors $\boldsymbol{b}^*_{\alpha(j)2}, j = 2, \ldots, p$. So any point of $\mathscr{k}_2(p)$ is described by a point from the cell $\mathscr{k}_2(p-1)$ whose center is shifted by the vector y_2 parallel to the vector $\boldsymbol{b}^*_{\alpha(1)2}$. Let z_2 be a fixed interior point of $\mathscr{k}_2(p)$ and construct the line

$$v_2(\mu) = z_2 + \mu\,\boldsymbol{b}^*_{\alpha(1)2}, \quad -\infty < \mu < \infty.$$

Since z_2 is an interior point of $\mathscr{k}_2(p)$, this line hits $s\,\mathscr{k}_2(\,)$ in two points corresponding to values $\mu = \underline{\mu}$, $\mu = \bar{\mu}$ with $\underline{\mu} < 0 < \bar{\mu}$, and all points of the line $v_2(\mu)$ for $\underline{\mu} < \mu < \bar{\mu}$ are interior point of $\mathscr{k}_2(p)$. Since z_2 can also be represented in the form of Eq. (*), the line $v_2(\mu)$ for any value of $\lambda_{\alpha(1)}$ must intersect with the shifted cell $\mathscr{k}_2(p-1)$. If this intersection would consist of a single point, it can easily be shown that by shifting it parallel to $\boldsymbol{b}^*_{\alpha(1)2}$ one would produce points on the boundary of $\mathscr{k}_2(p)$ only, contrary to what was shown for all points $v_2(\mu)$, $\underline{\mu} < \mu < \bar{\mu}$ including the point z_2. Therefore for any value $\lambda_{\alpha(1)}$ the intersection of the line $v_2(\mu)$ with the shifted cell $\mathscr{k}_2(p-1)$ consists of an interval bounded by two values $\mu_1(\lambda_{\alpha(1)}), \mu_2(\lambda_{\alpha(1)})$ such that

$$\underline{\mu} \leqq \mu_1 < \mu_2 \leqq \bar{\mu}.$$

Upon shifting the cell $\mathscr{k}_2(p-1)$, this interval is shifted with a fixed length $\mu_2 - \mu_1$ between two extremal and unique positions

$$\underline{\mu} = \mu_1(\lambda_{\alpha(1)}) \leftrightarrow \lambda_{\alpha(1)} = -1,$$
$$\mu_2(\lambda_{\alpha(1)}) = \bar{\mu} \leftrightarrow \lambda_{\alpha(1)} = 1.$$

Now by a simple analysis on the line one can easily show that there exists a number $\lambda_{\alpha(1)}$ such that

$$\underline{\mu} < \mu_1(\lambda_{\alpha(1)}) < 0 < \mu_2(\lambda_{\alpha(1)}) < \bar{\mu},$$
$$-1 < \lambda_{\alpha(1)} < 1.$$

The first relation implies that for the vector z_2 corresponding to $\mu = 0$ there is a vector z_2' which describes the same point as an interior point of the shifted cell $\mathscr{k}_2(p-1)$ referred to its center. The second relation assures that the shift y_2 of the center of this cell does not involve the extremal values of $\lambda_{\alpha(1)}$.

[1] P. Kramer and R. Neri, Acta Cryst. A **40,** 580 (1984).
[2] P. Kramer, Z. Naturforsch. **40 a,** 775 (1985).
[3] R. W. Haase, L. Kramer, P. Kramer, and H. Lalvani, to be published.
[4] J. Kepler, Strena seu de Nive Sexangula, in: Ges. Werke Bd. 4, ed. by M. Caspar, München ab 1938.
[5] J. Kepler, Harmonices Mundi Libri V, in: Ges. Werke Bd. 6, ed. by M. Caspar, München ab 1938.
[6] G. Kowalewski, Der Keplersche Körper und andere Bauspiele, K. F. Koehlers Antiquarium, Leipzig 1938.